# Effects of Time Lags on Transient Characteristics of a Nutrient Cycling Model

GIAN ITALO BISCHI
*Istituto di Biomatematica dell'Università, I-61029 Urbino, Italy*

*Received 26 July 1991; revised 16 August 1991*

---

ABSTRACT

A simple ecosystem with limiting nutrient cycling is modeled by chemostat equations with an integral term describing the continuous time lag involved in the process of nutrient regeneration from organic sediments. The same model has already been proposed in a previous paper, where conditions for boundedness of the solutions and stability of the equilibria were given. This paper is concerned with the relationships between resilience, that is, the speed with which the system returns to a stable equilibrium following a perturbation, and the time lag in the nutrient recycling process. Simple algorithms are given for the numerical calculation of the characteristic return time toward the stable equilibrium following a small perturbation. These methods also allow us to distinguish the case of monotone convergence from that of oscillatory convergence toward equilibrium. The numerical results obtained show that the presence of the time lag causes both qualitative and quantitative modifications in the dependence of equilibrium resilience on some relevant ecological parameters, such as the input nutrient concentration and the recycling extent. Analytical results for "quasi-closed" ecosystems are given that show that such stable systems are characterized by a very low resilience.

---

## 1. INTRODUCTION

Models of ecosystems with nutrient cycling have been studied by many authors, both for closed systems [3, 14, 15] and for open systems [5, 6, 13, 18]. Many of these results concern the effect of nutrient recycling on the existence and stability of equilibria [14; 15; 20, Ch. 5] and on relative stability measured in terms of resilience, that is, the rate at which a system returns to a stable equilibrium after a perturbation [5, 6, 13, 17].

A feature common to these papers is that nutrient recycling is assumed to be instantaneous, that is, the time required by the whole process of bacterial

---

Work performed within the activity of the research group Equazioni di Evoluzione Non Lineari in Biologia, MURST-Italy, and under the auspices of GNFM, CNR-Italy.

655 Avenue of the Americas, New York, NY 10010

0025-5564/92/$5.00

decomposition of dead biomass and waste organic products, together with the time necessary to recirculate the regenerated nutrients, is neglected. Nakajima and DeAngelis [13] emphasize that "this assumption is unrealistic," and Nisbet and Gurney [14] stress that even if this assumption seems to be reasonable in tropical and subtropical regions, time delays in the decomposition process cannot be neglected in boreal systems. May [11] also suggests that residence times and storage times should be considered when nutrient cycling effects on ecosystems are investigated.

In this paper, chemostat equations are used to model the growth of an autotroph species in the presence of a limiting nutrient that is partially recycled. Chemostat equations are widely used to model plankton communities in lakes (see, e.g., [9], [22], [19], [18]), but a substantial difference between a laboratory and a "lake" situation is that nutrients and sediments have much longer residence times in lakes [16, 18], that is, a smaller washout constant [19]. In such a situation detrital biomass accumulates and nutrient regeneration must be considered.

Some authors have introduced the detrital biomass as a dynamical variable [5, 21]. The equations describing detritus mineralization should account for many factors such as biomass sinking, burial in deep sediments, chemical reactions, bacterial activity, and, as pointed out in [21], oxygen concentration, with the possibility of switching from aerobic to anaerobic conditions. An alternative to this is to introduce a distributed time lag into the nutrient recycling term. In other words, all the processes involved in nutrient recycling are regarded as a whole by a distributed time lag with a delay kernel that gives the influence of the biomass of the past on the present nutrient concentration. This delay has been introduced in the chemostat equations as an integral term.

The resulting integrodifferential equations have already been considered in a previous paper [1], and the general results of boundedness and stability given there are summarized in Section 2, together with a description of the model equations and parameters. In Section 3 the resilience of the positive equilibrium is studied both for the model with instantaneous recycling and for the one containing distributed delay with a particular class of kernels. A simple algorithm for the numerical calculation of the characteristic return time is given, the dependence of the return time on the most relevant parameters is investigated, and the important role of the time lag in recycling is evidenced. The numerical results in Section 3 show that some parameters have a stabilizing effect (i.e., reduce the return time) when increased in some ranges and a destabilizing effect in other ranges. Thus, critical values of these parameters can be found in which resilience is maximum. These critical values are strongly influenced by the time lag and are characterized by a change from an oscillatory convergence toward the equilibrium to a monotone convergence after a small perturbation. The results given show that, in general, an increase of the recycling delay $T$ inhibits oscillations; increasing values of $T$ bring about a change from a situation of relatively fast oscillatory convergence to a slow monotone return to equilibrium. In Section 4 some approximate analytical expressions of the characteristic return time are given in the case of a very long residence time and a very tight recycling. These results indicate that for a sufficiently long time lag the return to equilibrium following a small perturbation is characterized by the absence of oscillations and by a low resilience.

## 2. THE MODEL

The ecosystem with delayed nutrient recycling is modeled by the following chemostat-type integrodifferential equations:

$$\dot{S} = D(S^\circ - S) - \gamma m_1 U(S) N + \gamma b D_1 \int_{-\infty}^{t} F(t-\tau) N(\tau)\, d\tau,$$

$$\dot{N} = N[-(D + D_1) + m_1 U(S)] \qquad (1)$$

where $S(t)$ is the concentration of a limiting nutrient at time $t$, $N(t)$ is the biomass of an autotroph species at time $t$, $S^\circ$ is the input concentration of the limiting nutrient, $D$ is the washout rate, $m_1$ is the maximum growth rate of the species, $D_1$ represents the loss rates from the living species (mortality and respiration), $\gamma$ is the constant ratio of nutrient mass to biomass (its inverse is usually called the yield constant), and $b \in [0,1]$ is the fraction of nutrient that is recycled from detritus. This parameter can be considered a measure of the extent of nutrient recycling within an open system because its value is mainly lowered by detritus washout as well as burial in deep sediments and the formation of insoluble nutrient compounds; $b = 0$ if no recycling occurs, and $b = 1$ if the recycling is complete, as in experiments with self-sustained closed ecosystems.

The function $U(S)$: $[0, +\infty) \to [0, 1)$ represents the nutrient uptake rate, and we assume that it is a continuously differentiable increasing function such that

$$U(0) = 0 \qquad \text{and} \qquad \lim_{S \to \infty} U(S) = 1. \qquad (2)$$

In particular, these hypotheses are satisfied by the familiar Michaelis–Menten function

$$U(S) = S/(A + S), \qquad (3)$$

where $A$ is the half-saturation constant. All the following results are given for a general uptake function satisfying hypotheses (2), but the numerical computations will be performed with function (3).

The delay kernel $F(u)$ is a nonnegative function defined on $[0, +\infty)$ and normalized; that is,

$$\int_0^\infty F(u)\,du = 1. \tag{4}$$

This function describes the rate at which the biomass losses of the past contribute to the available nutrient at time $t$. The average time lag of the recycling process is defined as

$$T := \int_0^\infty uF(u)\,du. \tag{5}$$

System (1) with initial conditions

$$S(0) = S_0 > 0; \qquad N(\tau) = \phi(\tau), \qquad -\infty < \tau \leqslant 0, \tag{6}$$

where $\phi$: $(-\infty, 0] \to \mathbb{R}_+$ is a bounded and (at least piecewise) continuous function, possesses a unique positive solution continuously dependent on parameters and initial data (see, e.g., [4]). Furthermore, we give the following theorem, which is a prerequisite for any reasonable model in ecology.

*THEOREM 1*

*All solutions $S(t)$, $N(t)$ of* (1) *with* (6) *are bounded for $t > 0$.*

This theorem can be proved following the procedure given by Beretta et al. [1]. System (1) has two nonnegative fixed points, $E_\circ = (S^\circ, 0)$ and $E_1 = (S_e, N_e)$, with

$$S_e = U^{-1}\left(\frac{D + D_1}{m_1}\right), \qquad N_e = \frac{D(S^\circ - S_e)}{\gamma[D + D_1(1-b)]}. \tag{7}$$

$E_1$ is positive provided that

$$(D + D_1) < m_1 \quad \text{and} \quad S^\circ > S_e. \tag{8}$$

In the following we deal only with local (linear) stability of the positive equilibrium $E_1$. Once linearized around $E_1$, the characteristic equation of the variational system is

$$\lambda^2 + (D + \gamma m_1 k)\lambda + \gamma m_1 k(D + D_1) - \gamma m_1 b D_1 k\, \mathscr{L}(\lambda) = 0, \tag{9}$$

where

$$k := U'(S_e) N_e \tag{10}$$

and $\mathscr{L}(\lambda)$ is the Laplace transform of the delay kernel (see, e.g., [10]).

In the following we consider a special class of kernels, the gamma distributions of integer order $p$:

$$F(u) = g_{\alpha,p}(u) = \frac{\alpha^{p+1}}{p!} u^p \exp(-\alpha u). \tag{11}$$

These functions are widely used in the ecological literature (see, e.g., [10] and references therein) and have the nice property that the characteristic equation (8) becomes an algebraic equation because the Laplace transform of $g_{\alpha,p}$ is

$$\mathscr{L}(\lambda) = \left(\frac{\alpha}{\alpha + \lambda}\right)^{p+1}. \tag{12}$$

The local stability of $E_1$ was studied in [1], where the following theorem is given.

*THEOREM 2*

*The positive equilibrium $E_1$ of system* (1) *with delay kernels* (11) *of arbitrary order $p \geqslant 0$ is always locally asymptotically stable.*

Because this stability result is important for the discussion on relative stability in the following sections, a sketch of the proof given in [1] is reported in the Appendix.

Theorem 2 states that the positive steady state is stable independently of the magnitude of the mean delay, which, from (5) with (11), is given by

$$T = (p + 1)/\alpha. \tag{13}$$

However, the relative stability of the equilibrium is strongly influenced by the time lag in recycling, as we shall see in the next section, where the cases of delay kernels (11) with $p = 0$ and $p = 1$ are considered. Following [4] I use the term "weak" kernel to denote one with $p = 0$ (the maximum of this kernel occurs at the present time, and past densities have exponentially decreasing influence) and "strong" kernel to denote one with $p = 1$ (the maximum occurs at the previous time, $t - T$).

## 3. RESILIENCE OF THE POSITIVE EQUILIBRIUM

Let $\lambda^*$ be the root of the characteristic equation (9) with the largest real part. When the equilibrium is stable all the eigenvalues lie in the left-half complex plane, so $\lambda^*$ is the root closest to the imaginary axis and dominates the long-term behavior of the system for initial conditions near equilibrium. This means that every solution of the variational system [and every solution of the original system (1) with initial conditions sufficiently close to $E_1$] tends to equilibrium at least as rapidly as $\exp[-|\mathrm{Re}(\lambda^*)|]t$, (see, e.g., [8]). Following [5] we call $\lambda^*$ the dominant eigenvalue and define the characteristic return time for the stable equilibrium as

$$T_r := -1/\mathrm{Re}(\lambda^*). \tag{14}$$

Then the equilibrium resilience can be defined as the inverse of the return time [5, 17]. Of course, this definition of resilience applies only to perturbations in a small region around the stable equilibrium where the nonlinear terms can be neglected.

We first discuss the case of instantaneous recycling: model (1) with $F(u) = \delta(u)$. Even if this assumption is unrealistic, the straightforward results obtained in this case can be used for comparison. The characteristic equation (9) becomes a simple second-degree algebraic equation:

$$\lambda^2 + (D + \gamma m_1 k)\lambda + \gamma m_1 k[D + D_1(1-b)] = 0. \tag{15}$$

This is the characteristic equation of a linear free oscillator with restoring force

$$\rho = \gamma m_1 k[D + D_1(1-b)] = m_1 D U'(S_e)(S^\circ - S_e) \tag{16}$$

and damping force proportional to

$$\eta = D + \gamma m_1 k = D\left[1 + \frac{m_1 U'(S_e)(S^\circ - S_e)}{D + D_1(1-b)}\right]. \tag{17}$$

Let $\Delta(b) := \eta^2(b) - 4\rho$. It can be easily proved (see Appendix) that for small values of the washout constant $D$ (i.e., in a "lake" situation), $\Delta(0) < 0$ and $\Delta(1) > 0$. On the basis of this result, and from the well-known elementary theory of linear oscillators, we have the following theorem.

*THEOREM 3*

*If $D$ is sufficiently small, a critical value $b_c \in (0,1)$ exists such that:*

(i) *If $0 < b < b_c$, then the system is "underdamped"; that is, it approaches the steady-state $E_1$ through oscillations of decreasing amplitude, and the characteristic return time is a decreasing function of $b$,*

$$T_r = 2/\eta(b).$$

(ii) *If $b_c < b < 1$, then the system is "overdamped"; that is, its return to the equilibrium is nonoscillatory, and the characteristic return time is an increasing function of $b$:*

$$T_r = \frac{2}{\eta(b) - \left[\eta(b)^2 - 4\rho\right]^{1/2}}.$$

Figure 1 shows the return time, computed according to Theorem 3, as the parameter $b$ varies in the range [0.5, 1] and the other parameters have the values listed in Table 1. Note that in almost the entire range of $b$, $T_r(b)$ is a decreasing function, so an increase in the recycling extent brings a higher resilience.

Numerically computed trajectories of model (1) with instantaneous recycling are shown in Figures 2a and 2b with $b < b_c$ and $b \simeq b_c$, respectively.

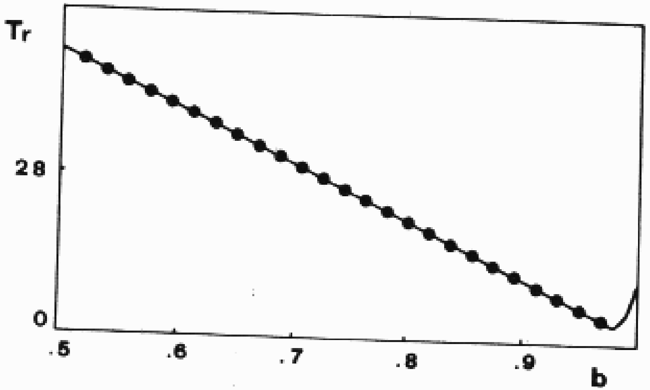

FIG. 1. Return time $T_r$ as a function of the recycling extent $b$ for model (1) with $F(u) = \delta(u)$, that is, instantaneous recycling. The other parameters have the values listed in Table 1. For $b < b_c = 0.98$, the eigenvalues are complex conjugate (●), whereas for $b > b_c$ a real eigenvalue is dominant (——).

TABLE I

Parameter Values Used in Numerical Calculations
(Unless Differently Specified)

| | | | |
|---|---|---|---|
| $D = 0.001$ | $b = 0.1$ | $A = 0.005$ | $S^\circ = 0.08$ |
| $D_1 = 0.1$ | $\gamma = 0.02$ | $m_1 = 0.3$ | |

*Note*. These parameter values have been taken from [5]. As pointed out in that paper, "these parameters are hypothetical and no units are assigned." However, these values form a plausible set for an aquatic system. Of course, any numerical results obtained with this set of parameters can give only qualitative informations.

If model (1) with delay kernels (11) of finite order $p$ is considered, the characteristic equation (9) becomes an algebraic equation of degree $n = p+3$:

$$\lambda^2(\alpha+\lambda)^{p+1} + (D+\gamma m_1 k)(\alpha+\lambda)^{p+1}\lambda + \gamma m_1 k(D+D_1)(\alpha+\lambda)^{p+1} - \gamma m_1 k b D_1 \alpha^{p+1} = 0. \qquad (18)$$

From Theorem 2 we know that all the roots of (18) lie in the left-half complex plane. In order to compute the distance of the dominant eigenvalue from the imaginary axis, we introduce in (18) a change of variable (as in [2] and [8]),

$$\lambda = z - \sigma, \qquad \sigma \in \mathbb{R}_+, \qquad (19)$$

to obtain an equation in the form

$$z^n + a_{n-1}(\sigma) z^{n-1} + \cdots + a_0(\sigma) = 0. \qquad (20)$$

This change of variable represents a shift of the imaginary axis to the left. If $\sigma^*$ is the greatest value of $\sigma$ such that all the roots $z_i$ of the transformed equation (20) lie in the left-half plane, then $\sigma^* = |\mathrm{Re}(\lambda^*)|$ and the characteristic return time for $E_1$ is $T_r = 1/\sigma^*$.

As all the roots have negative real parts when $\sigma = 0$ and the roots $z_i$ depend continuously on the parameter $\sigma$, a root will cross the imaginary axis for increasing $\sigma$ if and only if one of the two following cases occurs:

(1) $z = 0$ is a root of Equation (20) (in which case a real root crosses the imaginary axis), or

(2) $z = i\omega$, $\omega \in \mathbb{R}_+$, is a root of Equation (20) (in which case a pair of complex conjugate roots cross the imaginary axis).

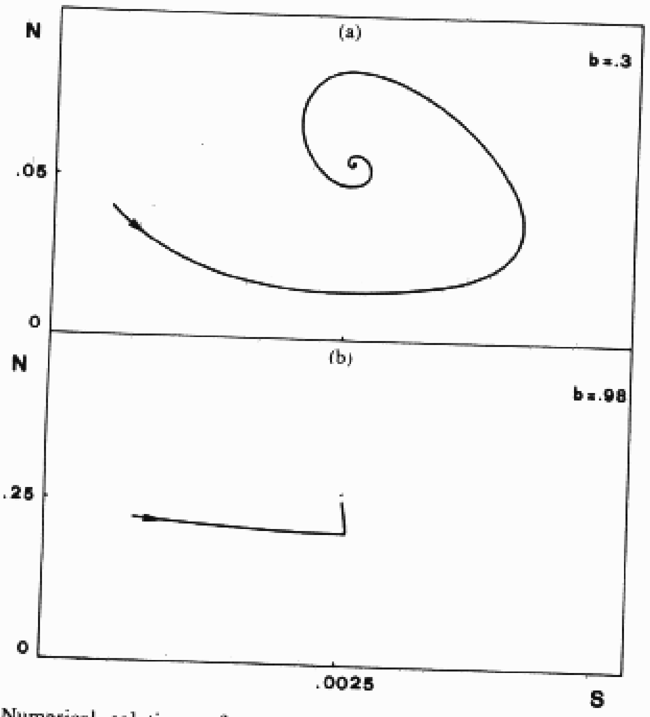

FIG. 2. Numerical solutions of model (1) with instantaneous recycling for two different values of parameter $b$: (a) $b = 0.3 < b_c$; (b) $b = 0.98 = b_c$. The other parameters have the same values as those used for Figure 1.

The first case occurs if and only if $a_0(\sigma) = 0$, the second if and only if $D_{n-1}(\sigma) = 0$, where $D_{n-1}$ is the Hurwitz determinant of order $n-1$. (The last statement is a consequence of a result of Orlando, which can be found in [7, Ch. 15] or [10, p. 71].) We first apply this argument to the case of delay kernel (11) with $p = 0$, the "weak" delay case. In this case the characteristic equation (18) becomes a third-degree equation,

$$\lambda^3 + C_2\lambda^2 + C_1\lambda + C_0 = 0 \qquad (21)$$

with

$$C_0 = \gamma m_1 k \alpha\left[D + D_1(1-b)\right] = D m_1 \alpha U'(S_e)(S^\circ - S_e), \qquad (22a)$$

$$C_1 = \alpha(D + \gamma m_1 k) + \gamma m_1 k(D + D_1), \qquad (22b)$$

$$C_2 = D + \gamma m_1 k + \alpha, \qquad (22c)$$

and the coefficients of the transformed equation (20) become

$$a_0(\sigma) = -\sigma^3 + C_2\sigma^2 - C_1\sigma + C_0, \tag{23a}$$

$$a_1(\sigma) = 3\sigma^2 - 2C_2\sigma + C_1, \tag{23b}$$

$$a_2(\sigma) = C_2 - 3\sigma. \tag{23c}$$

Let

$$\Delta_2(\sigma) = a_1(\sigma)a_2(\sigma) - a_0(\sigma). \tag{24}$$

The next two theorems are consequences of the argument outlined above. (Their proofs are in the Appendix.)

*THEOREM 4*

*Let* $\sigma_i$ *be the smallest real positive solution of the equation* $a_i(\sigma) = 0$, $i = 0, \ldots, 2$, *and* $\sigma_3$ *the smallest real positive solution of* $\Delta_2(\sigma) = 0$, *with the understanding that* $\sigma_i = +\infty$ *if the corresponding equation has no solutions. Then* $\sigma^* = \min(\sigma_i, i = 0, \ldots, 3)$.

Note that a lower bound for the characteristic return time can be obtained from each of the $\sigma_i$ computed according to this theorem. For example, $\sigma_2 = (D + \gamma m_1 k + \alpha)/3$ implies that $T_r$ lies above the hyperbola $T_r = 3T/[1 + (D + \gamma m_1 k)T]$ because $T_r = 1/\sigma^* \geqslant 1/\sigma_2$. In reality only two of the four equations appearing in Theorem 4 need be studied to find $\sigma^*$, according to the following theorem.

*THEOREM 5*

*Let* $\sigma_0$ *be the smallest real positive solution of the equation* $a_0(\sigma) = 0$ *and* $\sigma_3$ *the smallest real positive solution of* $\Delta_2(\sigma) = 0$, *with the understanding that* $\sigma_i = +\infty$ *if the corresponding equation has no solutions. Then* $\sigma^* = \min(\sigma_0, \sigma_3)$, *and when* $\sigma^* = \sigma_0$ *a real eigenvalue is dominant (thus giving a monotone or "overdamped" convergence) whereas when* $\sigma^* = \sigma_4$ *a pair of complex conjugate eigenvalues are dominant (oscillatory or "underdamped" convergence).*

From this theorem a simple algorithm can be derived for the numerical calculation of $T_r$ with a given set of model parameters. Starting from $\sigma = 0$, the first real root of the equation $a_0(\sigma) = 0$ and the first real root of

$\Delta_2(\sigma) = 0$ in the interval $(0, \sigma_2)$ are numerically computed, and the smaller of the two is taken for the computation of $T_r$.

Using this algorithm, the influence of the mean time delay $T$ on the resilience of the positive equilibrium $E_1$ has been investigated. In Figure 3 the computed values of $T_r$ are represented versus $b$, with $b \in (0, 1)$, for four different values of the mean delay $T$. These graphs can be compared with that of Figure 1, which corresponds to the case $T = 0$. It can be observed that for $T = 2$, $T = 10$, and $T = 20$, as well for $T = 0$, increasing values of $b$ in the region of oscillatory convergence, starting in $b = 0$, cause a slight increase in resilience, until a critical value $b_c$ is reached where the resilience is maximum. At this point a real eigenvalue becomes dominant, and a further increase in $b$ leads to a sharp loss in resilience. With greater delays the region of oscillatory convergence, characterized by decreasing $T_r(b)$, is narrowed, and it completely disappears for $T > 90$. These numerical results indicate that, owing to a considerable time lag in the nutrient recycling process, which may be a typical situation of boreal ecosystems [14], the resilience is lowered by an increase in the recycling extent and the system returns toward the stable equilibrium without oscillations. Conversely, when the recycling process is fast, such as in ecosystems of tropical

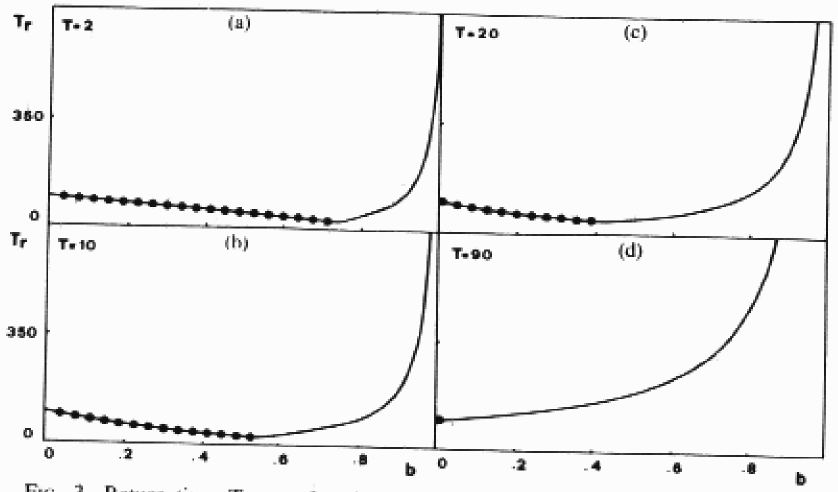

FIG. 3. Return time $T_r$ as a function of the recycling extent $b$ for model (1) with gamma delay kernels (11) with $p = 0$. The four graphs are obtained with different values of the mean time lag $T \doteq 1/\alpha$: (a) $T = 2$; (b) $T = 10$; (c) $T = 20$; (d) $T = 90$. The other parameter values are listed in Table 1. The curve with solid circles indicates that $\sigma^* = \sigma_3$, that is, a pair of complex conjugate eigenvalues are dominant (oscillatory convergence); the solid curve indicates that $\sigma^* = \sigma_0$, that is, a real eigenvalue is dominant (monotone convergence).

and subtropical regions [14], the convergence toward the equilibrium following a small perturbation is oscillatory and an increase in the recycling extent leads to a higher resilience.

In Figure 4 two numerical solutions of system (1) with the "weak" delay kernel are shown with a parameter set in the range where $\sigma^* = \sigma_3$ (Figure 4a) and where $\sigma^* = \sigma_0$ (Figure 4b). It can be noted that the stability domain of the positive equilibrium appears to be large, and our local resilience results are useful for larger perturbations as well.

In Figure 5, $T_r$ versus the input nutrient concentration $S°$ is shown with four different values of the mean delay $T$. In this case, too, increasing $T$ favors monotone convergence to equilibrium. However, when $S°$ is greater than the critical value, at which point there is the switch from underdamped to overdamped convergence, $T_r(S°)$ is almost a constant function. This is in agreement with the results of DeAngelis et al. [5], where $T_r$ is computed as a function of the nutrient input rate for a model with nutrient, autotroph, and detritus compartments using a method based on direct estimation of the return time during the computer simulations of the trajectories.

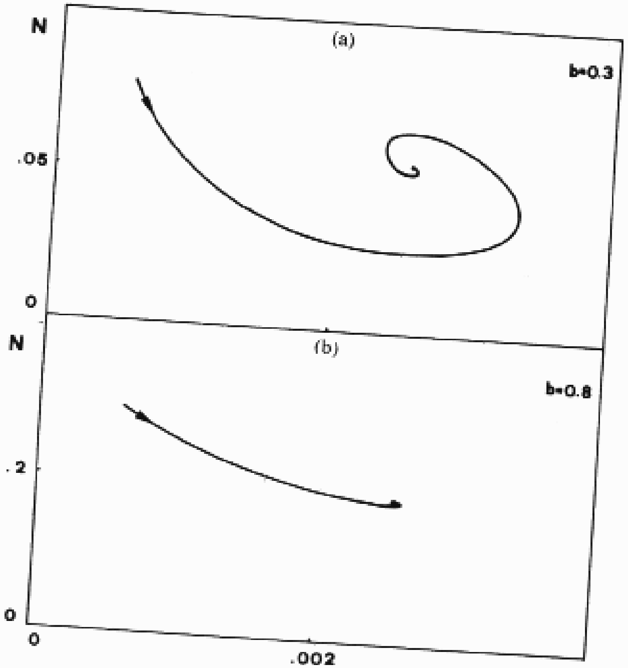

FIG. 4. Numerical solutions of model (1) with delay kernel (11) with $p = 0$ and $T = 10$. The numerical solutions are obtained by a Runge–Kutta method of order 4 applied to the expanded system of ordinary differential equations obtained by the linear chain trick (see, e.g., [10]). (a) $b = 0.3 < b_c$ ($\sigma^* = \sigma_3$ in this case); (b) $b = 0.8 > b_c$ ($\sigma^* = \sigma_0$ in this case). The other parameter values are listed in Table 1.

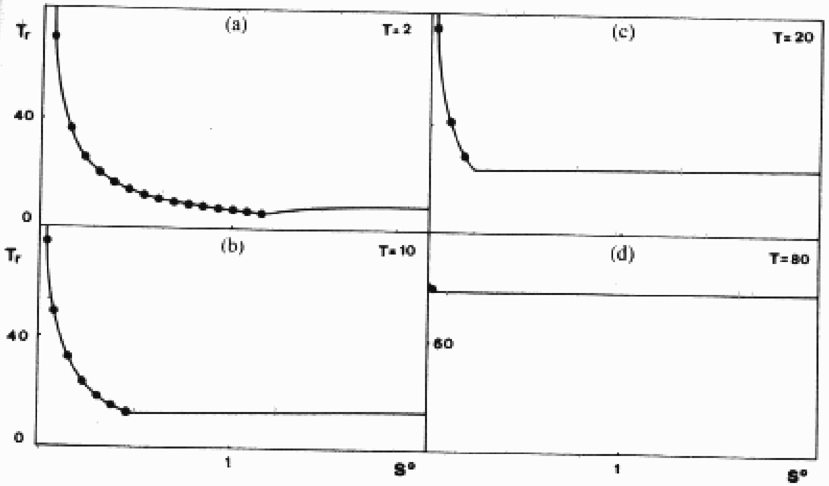

FIG. 5. Return time $T_r$ as a function of the nutrient input concentration $S°$ for model (1) with gamma delay kernels (11) with $p = 0$. The four graphs are obtained with different values of the mean time lag $T = 1/\alpha$: (a) $T = 2$; (b) $T = 10$; (c) $T = 20$; (d) $T = 90$. The other parameter values are listed in Table 1. The graphical symbols used in these curves have the same meaning as in Figure 3.

In Figure 6 the characteristic return time $T_r$ is represented versus the mean time lag $T$ with the other parameters fixed at the values listed in Table 1. In the first part of the graph, $T_r(T)$ is a decreasing function; thus in this range increasing time delays have a stabilizing effect. This graph also shows a nonmonotonic behavior of $T_r$, and a critical value of $T$ exists where $T_r$ is minimum; however, this does not correspond to the change between the dominance of the complex eigenvalues and that of the real eigenvalue, whereas this seemed to be the rule in previous cases. In other words, the maximum resilience, as $T$ varies, is not obtained at the point of switching from underdamped to overdamped convergence. As $T$ further increases, the real eigenvalue becomes dominant, and this leads to a faster loss of resilience.

The corresponding trajectories of the complex roots of the characteristic equation (21) are shown in Figure 7. At first the pair of dominant complex eigenvalues move away from the imaginary axis as $T$ increases. Then, before the real eigenvalue moving from the left becomes dominant, the pair of complex eigenvalues begin to slowly approach the imaginary axis.

Theorem 5 can be easily extended to the case of kernels (11) of higher

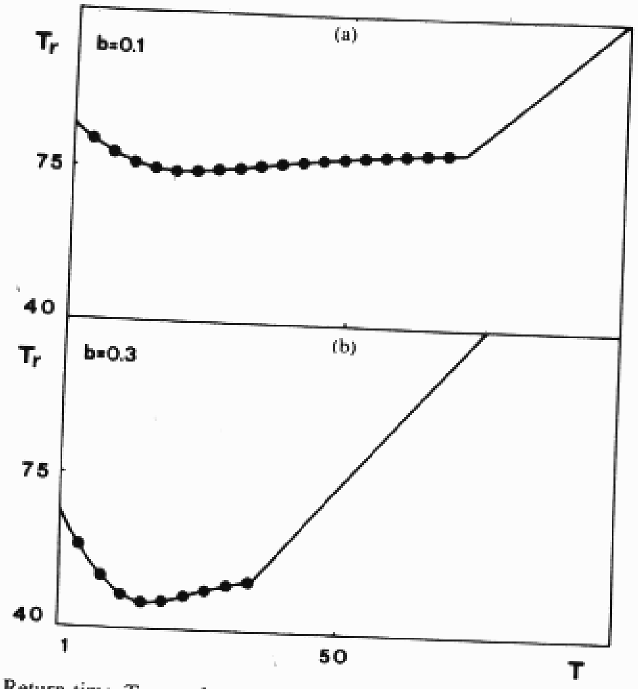

FIG. 6. Return time $T_r$ as a function of the mean time lag in the recycling process $T$ for model (1) with gamma delay kernels (11) with $p = 0$. The two graphs are obtained with different values of recycling extent $b$: (a) $b = 0.1$; (b) $b = 0.3$. The other parameter values are listed in Table 1. The graphical symbols used in these curves have the same meaning as in Figures 3 and 5.

order. If $p = 1$, then the characteristic equation becomes

$$\lambda^4 + C_3\lambda^3 + C_2\lambda^2 + C_1\lambda + C_0 = 0 \tag{25}$$

with

$$C_0 = \alpha^2\gamma m_1 k[D + D_1(1-b)] = \alpha^2 D m_1 U'(S_e)(S^\circ - S_e), \tag{26a}$$

$$C_1 = \alpha^2(D + \gamma m_1 k) + 2\alpha\gamma m_1 k(D + D_1), \tag{26b}$$

$$C_2 = \alpha^2 + 2\alpha(D + \gamma m_1 k) + \gamma m_1 k(D + D_1), \tag{26c}$$

$$C_3 = D + \gamma m_1 k + 2\alpha. \tag{26d}$$

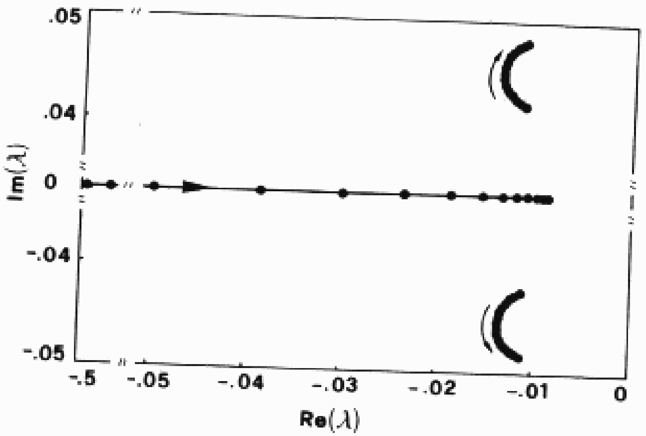

FIG. 7. Trajectories on the complex plane of the roots of the characteristic equation (21) as $T$ varies from 1 to 100. All the parameter values are the same as in Figure 6a.

The transformed equation, after the change of variable (19), is

$$z^4 + a_3(\sigma)z^3 + a_2(\sigma)z^2 + a_1(\sigma)z + a_0(\sigma) = 0 \tag{27}$$

with

$$a_0(\sigma) = \sigma^4 - C_3\sigma^3 + C_2\sigma^2 - C_1\sigma + C_0, \tag{28a}$$

$$a_1(\sigma) = -4\sigma^3 + 3C_3\sigma^2 - 2C_2\sigma + C_1, \tag{28b}$$

$$a_2(\sigma) = 6\sigma^2 - 3C_3\sigma + C_2, \tag{28c}$$

$$a_3(\sigma) = C_3 - 4\sigma. \tag{28d}$$

Let

$$\Delta_3(\sigma) := a_1(\sigma)a_2(\sigma)a_3(\sigma) - a_1(\sigma)^2 - a_0(\sigma)a_3(\sigma),$$

and let $\sigma_0$ be the smallest real positive root of $a_0(\sigma) = 0$ and $\sigma_4$ the smallest real positive root of $\Delta_3(\sigma) = 0$. [We can set $\sigma_i = +\infty$, $i = 0, \dots, 4$, if no real solutions of the corresponding equation exist in the interval $(0, \sigma_3)$, with $\sigma_3 = (D + \gamma m_1 k + 2\alpha)/4$.] In analogy to the case with $p = 0$, we have $\sigma^* = \min(\sigma_0, \sigma_4)$, and then $T_r = 1/\sigma^*$. Furthermore, if $\sigma^* = \sigma_0$, then a real eigenvalue is dominant, whereas if $\sigma^* = \sigma_4$, a pair of complex conjugate eigenvalues are dominant.

The results of some numerical computations of $T_r$ with $p = 1$ (“strong” delay) are shown in the Figures 8–10. The dependence of $T_r$ on the

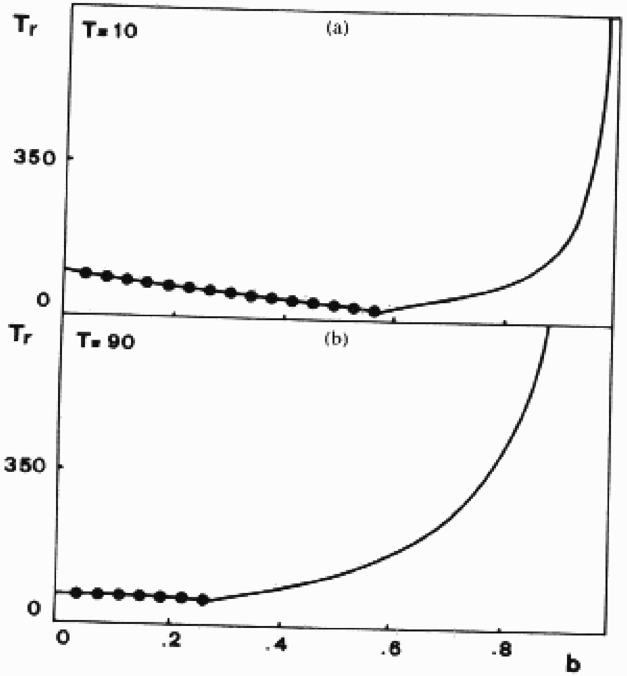

FIG. 8. Return time $T_r$ as a function of the recycling extent $b$ for model (1) with gamma delay kernels (11) with $p = 1$. The two graphs are obtained with different values of the mean time lag $T = 2/\alpha$: (a) $T = 10$; (b) $T = 90$. All other conditions are the same as in Figure 3, to which this figure should be compared. The curve with solid circles indicates that $\sigma^* = \sigma_3$; that is, a pair of complex conjugate eigenvalues are dominant (oscillatory convergence); the solid curve indicates that $\sigma^* = \sigma_0$, that is, a real eigenvalue is dominant (monotone convergence).

parameters $b$ and $S^\circ$ is not qualitatively changed in comparison to the case of "weak" delay. However, we can see that for a given value of $T = 2/\alpha$ the region in the parameter space characterized by oscillatory convergence is slightly enlarged. The fact that increasing order $p$ of the kernels (11) favors the oscillatory behavior of the system had been already stressed in [1] on the basis of some computer simulations. This tendency is particularly evidenced by the plots of $T_r(T)$ in Figure 10 compared to those in Figure 6. It can also be noticed that the minimum value of the return time in each graph of Figure 10 is less than that in the corresponding graph of Figure 6; that is, the "strong" kernel gives a higher relative stability characterized by oscillatory convergence.

Both in Figure 6 and in Figure 10 a higher value of the parameter $b$ inhibits the oscillatory behavior and gives a linearly increasing return time for great delays. This conjecture will be discussed analytically in the next section.

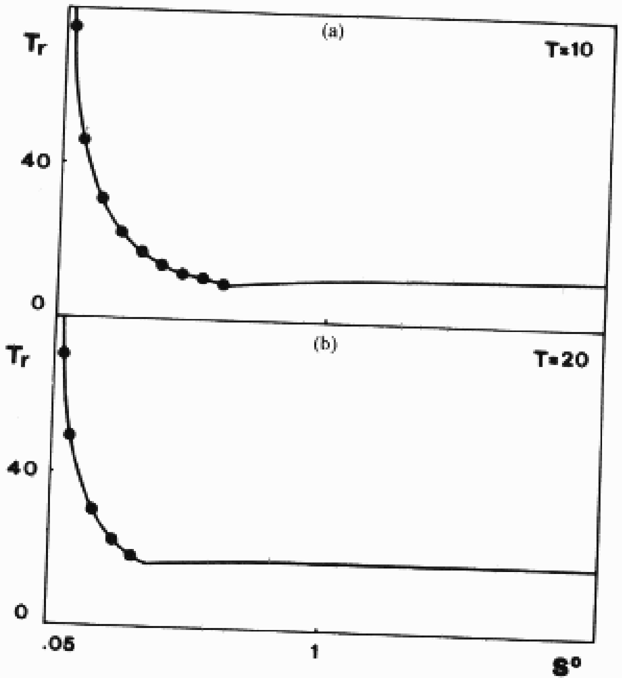

FIG. 9. Return time $T_r$ as a function of the nutrient input concentration $S^\circ$ for model (1) with gamma delay kernels (11) with $p = 1$. The two graphs are obtained with different values of the mean time lag $T = 2/\alpha$: (a) $T = 10$; (b) $T = 90$. All other conditions are the same as in Figure 5, to which this figure should be compared.

## 4. HYPOTHESIS OF HIGH DEGREE OF RECYCLING AND THE LIMIT OF CLOSED ECOSYSTEMS

The inverse of the washout constant, $1/D$, has the physical dimension of time and represents the residence time, that is, the average time that nutrients and waste products spend in the system [19]. A long residence time, that is, a small value of $D$, is a necessary condition for nutrient recycling. Thus the parameter $b$, which in model (1) is a measure of the recycling extent, is to some extent related to $D$ because a small value of $D$ generally implies a large value of $b$. This is not always true, because the recycling extent may also be lowered by other factors, such as burial in deep sediments or chemical reactions that cause the formation of insoluble compounds.

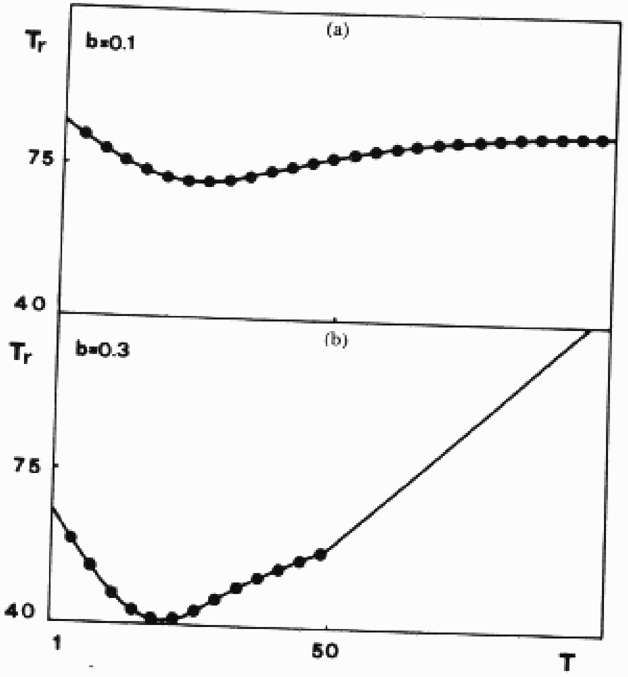

FIG. 10. Return time $T_r$ as a function of the mean time lag $T$ for model (1) with gamma delay kernels (11) with $p = 1$. The two graphs are obtained with different values of the recycling extent $b$: (a) $b = 0.1$; (b) $b = 0.3$. All other conditions are the same as in Figure 6, to which this figure should be compared.

In this section we assume that the nutrient recycling is hindered only by sediments washout. To simulate a long residence time we write

$$D := \epsilon D_0 \tag{29}$$

and, on the basis of the previous assumption,

$$b := 1 - \epsilon b_0, \tag{30}$$

where $\epsilon \ll 1$ and $D_0$, $b_0$ are positive constants.

Small $\epsilon$ implies that the residence time is much longer than the nutrient recycling time, so nutrient molecules are recycled many times before they leave the system. The limit $\epsilon = 0$ means that the system is closed, because in this case (29) implies $D = 0$. With this hypothesis the system can exist in a feasible steady state if and only if the recycling is complete, that is, $b = 1$.

In this case the total amount of nutrient in the system,

$$N_T = S(t) + \gamma N(t) + \gamma D_1 \int_0^{\infty} F(x) \left[ \int_{t-x}^{t} N(u)\, du \right] dx, \tag{31}$$

is constant [the last term in (31) can be interpreted as the amount of nutrient that is temporarily stored in the sediments].

From (7), with (29) and (30), we deduce that the biomass at equilibrium does not depend on $\epsilon$,

$$N_e = \frac{D_0(S^\circ - S_e)}{\gamma(D_0 + D_1 b_0)}, \tag{32}$$

and the nutrient equilibrium concentration is well approximated, for $\epsilon \ll 1$, by

$$S_e \simeq U^{-1}\left(\frac{D_1}{m_1}\right), \qquad D_1 < m_1. \tag{33}$$

We first consider the case of a "weak" delay kernel. From (29) and (30) the coefficients (22) of the characteristic equation can be considered as functions of $\epsilon$. In particular, $C_0$ is of order $\epsilon$ and can be written as

$$C_0 := \epsilon \overline{C}_0 \tag{34}$$

with

$$\overline{C}_0 = D_0 m_1 \alpha U'(S_e)(S^\circ - S_e). \tag{35}$$

This allows us to find an analytical approximation of the roots for $\epsilon \ll 1$ following the procedure given in [6] and [13]. The roots of the characteristic equation depend continuously on $\epsilon$, and for $\epsilon = 0$ a real root $\bar{\lambda}(0) = 0$ exists because $C_0(0) = 0$.

For small $\epsilon$ we can write

$$\bar{\lambda}(\epsilon) = \beta\epsilon + O(\epsilon^2). \tag{36}$$

Substituting (36) into the characteristic equation and taking only terms of first order in $\epsilon$, we obtain $\beta = -\overline{C}_0 / C_1(0)$. Thus a good approximation of $\bar{\lambda}$ is

$$\bar{\lambda}(\epsilon) = -\frac{\alpha(D_0 + D_1 b_0)}{\alpha + D_1}\epsilon = -\frac{D_0 + D_1 b_0}{1 + D_1 T}\epsilon. \tag{37}$$

For a given $\epsilon > 0$, $\bar{\lambda}$ is the dominant eigenvalue for great delay values. Thus for sufficiently high $T$ or small $\epsilon$ the characteristic return time is well approximated by

$$T_r = \frac{1}{|\bar{\lambda}|} = \frac{1 + D_1 T}{\epsilon(D_0 + D_1 b_0)}. \tag{38}$$

This result is in agreement with the conclusions of DeAngelis in [6] as both a decrease in the washout constant (i.e., a small $\epsilon$) and an increase in $T$ lead to a higher transit time of nutrients in the system.

For a given $T$, if $\epsilon \to 0$, that is, in the limit of closed ecosystems, $T_r \to +\infty$. This means that even if the equilibrium of a "quasi-closed" system is stable its resilience is extremely low. This may be an answer to the question raised in [15], where the authors try to reconcile the observed vulnerability of materially closed experimental ecosystems with the numerous demonstrations of stability in mathematical models of closed systems with material cycling. Our results, like those given in [6], state that if model (1) is "quasi-closed" it has a positive stable equilibrium but very low resilience. This means that the system will stay out of the steady state for a long time after a perturbation, which implies a high vulnerability.

For small values of $T$, the real eigenvalue (37) must be compared with the real part of the solutions of the second-degree equation

$$\lambda^2 + C_2(0)\lambda + C_1(0) = 0, \tag{39}$$

which is obtained by keeping the terms of zeroth order in $\epsilon$ in the characteristic equation.

The following theorem states that the reasoning given above can be applied if delay kernels (11) of arbitrary order $p \geqslant 0$ are considered and the approximated expression of the real eigenvalue $\bar{\lambda}$ given in (37) holds for each $p$.

*THEOREM 6*

*For each $p \geqslant 0$, if $\epsilon \ll 1$ or if $T = (p+1)/\alpha$ is sufficiently large, then the dominant eigenvalue of the characteristic equation* (18) *is well approximated by*

$$\bar{\lambda}(\epsilon) = -\frac{D_0 + D_1 b_0}{1 + D_1 T}\epsilon.$$

The proof is in the Appendix.

## 5. DISCUSSION

The present paper aims at investigating the effects of the time delay involved in nutrient recycling on resilience, that is, the rate at which a system returns to a stable steady state following a perturbation. This analysis has been carried out using the simple and general chemostat model (1) where an integral term has been inserted to represent the delayed recycling of the limiting nutrient. It has been proved that the positive equilibrium is stable, independently of delay magnitude, for a particular class of delay kernels. Thus the equilibrium resilience has been quantified as proportional to the absolute value of the real part of the dominant eigenvalue in the linear variational system.

A method has been given for the numerical calculation of the real part of the dominant eigenvalue without having to find the complex roots of the characteristic equation. This method also allows us to distinguish the case of a real dominant eigenvalue (monotone or "overdamped" convergence to equilibrium) from that of a pair of complex conjugate eigenvalues (oscillatory or "underdamped" convergence).

From the numerical results obtained, the dependence of resilience on the recycling extent appears to be nonmonotonic, and a critical value of the parameter $b$ exists at which the resilience is maximum and the type of convergence changes from oscillatory to nonoscillatory for increasing $b$. The critical value of $b$ decreases with increasing time lags; that is, increasing delays in recycling favor a destabilizing influence of $b$.

A counterintuitive result may be that an increase in the time lag inhibits the oscillatory behavior of the system, whereas it is a common belief that the presence of time lags causes oscillations [12]. Our results show that increasing time delays lead from a relatively fast oscillatory convergence to a slow monotone convergence, that is, the time lag in recycling acts as a damping force. However, when the system is characterized by oscillatory behavior (i.e., for small $T$), an increase in the time delay can have a stabilizing effect (this is another counterintuitive result).

The influence of the input nutrient concentration on resilience has also been studied, and for a small delay our results are in agreement with those given in [5]. In fact, for low values of $S°$ an increase in this parameter leads to a higher relative stability, whereas resilience seems to be practically independent of $S°$ for higher values of this parameter. In this case, too, the influence of the delay is evident as increasing the value of $T$ leads to a decrease in resilience and an extension of the domain where resilience is insensitive to $S°$ variations.

The analytical approximation of the dominant eigenvalue in the case of a "quasi-closed" ecosystem with strong recycling given in Section 4 shows that the stable equilibrium of such systems is characterized by low resilience and the characteristic return time is proportional to the delay in recycling. These results are consistent with the statement of DeAngelis in [6] that resilience is inversely related to the mean transit time, the mean time a unit of nutrient spends in the system from input to output.

The results obtained are confirmed by numerical simulations of the trajectories in the phase space of model (1). From these computer simulations the stability domain of the positive equilibrium appears to be very large, whereas the results given in the present paper apply only to small perturbations around the stable equilibrium, because they are obtained from the linear approximation of model (1). This is a shortcoming of the present work, and some effort should be devoted to the problem of return time for larger perturbations that bring the system into regions of the phase space where the nonlinear terms cannot be neglected. This question is rarely discussed in the literature and is worthy of attention in ecological problems.

## APPENDIX

### *PROOF OF THEOREM 2*

To prove that the roots of the $(p+3)$th-degree characteristic equation (18) are in the left-half complex plane for each $p \geqslant 0$, we use the method of mathematical induction. For $p=0$ the roots have negative real parts for each parameter value, because in this case the characteristic equation is the third-degree equation (21) whose coefficients (22) are all positive and such that

$$\begin{aligned} C_1C_2 - C_0 = {} & \alpha(D+\gamma m_1 k)(D+\gamma m_1 k+\alpha) \\ & + \gamma m_1 k(D+D_1)(D+\gamma m_1 k)+\gamma m_1 k \alpha b D_1 > 0. \end{aligned} \tag{A1}$$

Thus, from the Routh–Hurwitz criterion, every root of (21) has a strictly negative real part. We now suppose that this is true for Equation (18) with a given $p>0$ too. This means that no root can be on the imaginary axis; that is, Equation (18) with $\lambda = i\omega$, $\omega \in \mathbb{R}_+$,

$$\begin{aligned} & -\omega^2(\alpha+i\omega)^{p+1}+(D+\gamma m_1 k)i\omega(\alpha+i\omega)^{p+1} \\ & \quad +\gamma m_1(D+D_1)k(\alpha+i\omega)^{p+1}-\gamma m_1 b D_1 k \alpha^{p+1}=0, \end{aligned} \tag{A2}$$

is never satisfied.

Following [10, Ch. 9], we introduce a new variable $\theta$ such that $\tan\theta = \omega/\alpha$, $0<\theta<\pi/2$. Thus (A2) becomes

$$\begin{aligned} & e^{i(p+1)\theta}\left[-\omega^2+\gamma m_1(D+D_1)k+i(D+\gamma m_1 k)\omega\right] \\ & \quad = \gamma m_1 b D_1 k(\cos\theta)^{p+1}, \end{aligned} \tag{A3}$$

and, by taking the square modulus of both sides of (A3) we obtain the equation

$$\begin{aligned} & R(\omega) = (\cos\theta)^{p+1}, \quad \text{with} \\ & R(\omega) = \frac{\left[\gamma m_1(D+D_1)k-\omega^2\right]^2+(D+\gamma m_1 k)^2\omega^2}{\gamma^2 m_1^2 b^2 D_1^2 k^2}, \end{aligned} \tag{A4}$$

which cannot be satisfied for $\omega \in \mathbb{R}_+$.

Since $R(0) = [(D+D_1)/bD_1]^2 > 1$, it must be that $R(\omega) > (\cos\theta)^{p+1}$ for each $\omega > 0$. The same inequality is true for $p+1$; that is, $R(\omega) > (\cos\theta)^{p+2}$, $\omega \in \mathbb{R}_+$, because $0 \leqslant \cos\theta \leqslant 1$. So in this case too, no root can cross the imaginary axis as some parameter varies, and the thesis follows.

### *PROOF OF THEOREM 3*

Let us write

$$D := \epsilon D_0 \tag{A5}$$

with $\epsilon \ll 1$. After substitution of (A5) into (16) and (17), we have

$$\Delta(b) = \epsilon D_0\left[\epsilon D_0\left(1+\frac{m_1 U'(S_e)(S^\circ - S_e)}{\epsilon D_0 + D_1(1-b)}\right)^2 - 4m_1 U'(S_e)(S^\circ - S_e)\right], \tag{A6}$$

where the definition of $k$, Equation (10), has been used.

We have

$$\Delta(0) = \epsilon D_0\left[\epsilon D_0\left(1+\frac{m_1 U'(S_e)(S^\circ - S_e)}{\epsilon D_0 + D_1}\right)^2 - 4m_1 U'(S_e)(S^\circ - S_e)\right], \tag{A7}$$

which is negative for sufficiently small $\epsilon$, and

$$\Delta(1) = \epsilon D_0\left[\frac{\left[\epsilon D_0 + m_1 U'(S_e)(S^\circ - S_e)\right]^2}{\epsilon D_0} - 4m_1 U'(S_e)(S^\circ - S_e)\right], \tag{A8}$$

which is positive for sufficiently small $\epsilon$.

As $\Delta(b)$ is a continuous and increasing function of $b \in [0,1]$, a unique value $b_c \in (0,1)$ exists such that $\Delta(b_c) = 0$.

### *PROOF OF THEOREM 4*

After the change of variable, Equation (19), the characteristic equation (21) becomes

$$z^3 + a_2(\sigma)z^2 + a_1(\sigma)z + a_0(\sigma) = 0, \tag{A9}$$

with $a_i(\sigma)$, $i=0,\dots,2$, given in (23). From the generalization of Liénard and Chipart of the Routh–Hurwitz criterion (see, e.g., [7]), the conditions

$$a_i(\sigma) > 0, \quad i = 0,\dots,2, \qquad \text{and} \qquad \Delta_2(\sigma) > 0 \tag{A10}$$

with $\Delta_2$ given by (24), are necessary and sufficient for all the roots of (A9) to have negative real parts. These conditions are satisfied for $\sigma = 0$ because in this case (A9) is identical to (21). When the parameter $\sigma$ increases (i.e., the imaginary axis shifts to the left), the minimum positive $\sigma$ at which at least one of the inequalities (A10) is not satisfied represents the first value of $\sigma$ at which at least one root crosses the imaginary axis. This value of $\sigma$ is $\sigma^*$, the distance of the dominant eigenvalue from the imaginary axis. This completes the proof.

### PROOF OF THEOREM 5

This is a straightforward consequence of a result of Orlando (see, e.g., [10, p. 71] or [7]) together with the continuous dependence of the roots on parameter $\sigma$. However, in our case it can be proved very easily. If $a_0(\sigma) = 0$, then $z = 0$ is a root of (A9), and vice versa. Furthermore, $z = \pm i\omega$, $\omega \in \mathbb{R}_+$, are roots of (A9) if and only if the real and the imaginary parts of (A9) vanish, that is,

$$-a_2(\sigma)\omega^2 + a_0(\sigma) = 0 \quad \text{and} \quad \omega\left[a_1(\sigma) - \omega^2\right] = 0. \tag{A11}$$

Substituting for $\omega^2$ in the second equation gives $-\Delta_2(\sigma)/a_2(\sigma)^2 = 0$.

### PROOF OF THEOREM 6

The characteristic equation (18) with parameters $D$ and $b$ given by (29) and (30) can be written as

$$\lambda^{p+3} + C_{p+2}(\epsilon)\lambda^{p+2} + \cdots + C_1(\epsilon)\lambda + C_0(\epsilon) = 0, \tag{A12}$$

with

$$C_0(\epsilon) = \epsilon\alpha^{p+1}D_0 m_1 U'(S_e)(S^\circ - S_e) := \epsilon\bar{C}_0 \tag{A13}$$

and

$$\bar{C}_1(\epsilon) = (\epsilon D_0 + \gamma m_1 k)\alpha^{p+1} + \gamma m_1 k(\epsilon D_0 + D_1)(p+1)\alpha^p. \tag{A14}$$

Let $\bar{\lambda}(\epsilon)$ be the root such that $\bar{\lambda}(0) = 0$. Following the same reasoning as in Section 4, a good approximation of $\bar{\lambda}(\epsilon)$ for $\epsilon \ll 1$ is

$$\bar{\lambda}(\epsilon) = -\frac{\bar{C}_0}{\bar{C}_1(0)}\epsilon = -\frac{\alpha^{p+1}D_0 m_1 U'(S_e)(S^\circ - S_e)}{\gamma m_1 k\alpha^p\left[\alpha + (p+1)D_1\right]}\epsilon = -\frac{D_0 + D_1 b_0}{1 + D_1 T}\epsilon, \tag{A15}$$

where the definition [Eq. (10)] of $k$ and $\alpha = (p+1)/T$ have been used.

## REFERENCES

1 E. Beretta, G. I. Bischi, and F. Solimano, Stability in chemostat equations with delayed nutrient recycling, *J. Math. Biol.* 28:99–111 (1990).

2 F. Brauer, Decay rates for solution of a class of differential-difference equations, *SIAM J. Math. Anal.* 10:783–788 (1979).

3 S. Busenberg, S. K. Kumar, P. Austin, and G. Wake, The dynamics of a model of a plankton–nutrient interaction, *Bull. Math. Biol.* 52:677–696 (1990).

4 J. M. Cushing, *Integrodifferential Equations and Delay Models in Population Dynamics* (Lect. Notes Biomath., 20), Springer-Verlag, New York, 1977.

5 D. L. DeAngelis, S. M. Bartell, and A. L. Brenkert, Effects of nutrient recycling and food-chain length on resilience, *Am. Nat.* 134:778–805 (1989).

6 D. L. DeAngelis, Energy flow, nutrient cycling, and ecosystem resilience, *Ecology* 61:764–771 (1980).

7 F. R. Gantmacher, *The Theory of Matrices*, Vol. 2, Chelsea, New York, 1959.

8 K. Gopalsamy, Harmless delays in model systems, *Bull. Math. Biol.* 45:295–309 (1983).

9 S. B. Hsu, S. Hubbel, and P. Waltman, A mathematical theory for single-nutrient competition in continuous cultures of micro-organisms, *SIAM J. Appl. Math.* 32:366–383 (1977).

10 N. MacDonald, *Biological Delay Systems: Linear Stability Theory*, Cambridge Univ. Press, Cambridge, 1989.

11 R. M. May, A cycling index for ecosystems, *Nature* 292:105 (1981).

12 J. Maynard Smith, *Models in Ecology*, Cambridge Univ. Press, Cambridge, 1974.

13 H. Nakajima and D. L. DeAngelis, Resilience and local stability in a nutrient-limited resource–consumer system, *Bull. Math. Biol.* 51:501–510 (1989).

14 R. M. Nisbet and W. S. C. Gurney, Model of material cycling in a closed ecosystem, *Nature* 264:633–635 (1976).

15 R. M. Nisbet, J. McKinstry, and W. S. C. Gurney, A "strategic" model of material cycling in a closed ecosystem, *Math. Biosci.* 64:99–113 (1983).

16 E. P. Odum, *Fundamentals of Ecology*, Saunders, Philadelphia, 1971.

17 S. L. Pimm, *Food Webs*, Chapman & Hall, London, 1982.

18 T. Powell and P. J. Richerson, Temporal variation, spatial heterogeneity and competition for resources in plankton systems: a theoretical model, *Am. Nat.* 125:431–464 (1985).

19 H. L. Smith, Competitive coexistence in an oscillatory chemostat, *SIAM J. Appl. Math.* 32:366–383 (1977).

20 Y. M. Svirezhev and D. O. Logofet, *Stability of Biological Communities*, Mir, Moscow, 1983.

21 A. A. Voinov and Y. M. Svirezhev, A minimal model of eutrophication in freshwater ecosystems, *Ecol. Modelling* 23:277–292 (1984).

22 P. Waltman, S. P. Hubbel, and S. B. Hsu, Theoretical and experimental investigation of microbial competition in continuous cultures, in *Modeling and Differential Equations in Biology*, T. Burton, ed., Marcel Dekker, New York, 1980.